Neurobiology of Aging xxx (2015) 1–10

Contents lists available at ScienceDirect

Neurobiology of Aging

journal homepage: www.elsevier.com/locate/neuaging

JNK-interacting protein 1 mediates Alzheimer's-like pathological features in AICD-transgenic mice

Daniel R. Margevicius [a,b,*], Chinthasagar Bastian [a], Qingyuan Fan [a], Roger J. Davis [c], Sanjay W. Pimplikar [a,b]

[a] Department of Neurosciences, Lerner Research Institute, The Cleveland Clinic, Cleveland, OH, USA
[b] Department of Molecular Medicine, Case Western Reserve University, Cleveland, OH, USA
[c] Program in Molecular Medicine, University of Massachusetts Medical School and Howard Hughes Medical Institute, Worcestor, MA, USA

ARTICLE INFO

Article history:
Received 25 September 2014
Received in revised form 21 April 2015
Accepted 23 April 2015

Keywords:
Alzheimer's
APP
AICD
JNK
JNK-interacting protein 1
Tau

ABSTRACT

Amyloid precursor protein, which generates amyloid beta peptides, is intimately associated with Alzheimer's disease (AD) pathogenesis. We previously showed that transgenic mice overexpressing amyloid precursor protein intracellular domain (AICD), a peptide generated simultaneously with amyloid beta, develop AD-like pathologies, including hyperphosphorylated tau, loss of synapses, and memory impairments. AICD is known to bind c-Jun N-terminal kinase (JNK)–interacting protein 1 (JIP1), a scaffold protein that associates with and activates JNK. The aim of this study was to examine the role of JIP1 in AICD-induced AD-like pathologies in vivo, since the JNK pathway is aberrantly activated in AD brains and contributes to AD pathologies. We generated AICD-Tg mice lacking the JIP1 gene (AICD; JIP1$^{-/-}$) and found that although AICD; JIP1$^{-/-}$ mice exhibit increased AICD, the absence of JIP1 results in decreased levels of hyperphosphorylated tau and activated JNK. AICD; JIP1$^{-/-}$ mice are also protected from synaptic loss and show improved performance in behavioral tests. These results suggest that JIP1 mediates AD-like pathologies in AICD-Tg mice and that JNK signaling may contribute to amyloid-independent mechanisms of AD pathogenesis.

1. Introduction

Alzheimer's disease (AD) is a slowly progressing neurodegenerative disorder of unknown etiology. It is characterized by extracellular accumulations of beta-amyloid (Aβ) peptides derived from proteolytic processing of the amyloid precursor protein (APP), intracellular accumulations of hyperphosphorylated microtubule–associated protein tau, and neurodegeneration (Goate and Hardy, 2012; Selkoe, 2008). Although the predominant model of AD pathogenesis posits that increased levels of Aβ peptides are the primary cause of AD (Hardy and Selkoe, 2002; Selkoe, 2008), it is becoming increasingly clear that AD is likely to be a multifactorial, heterogeneous disease and that alternative, nonamyloid-based mechanisms also likely contribute to AD pathogenesis (Pimplikar, 2009; Pimplikar et al., 2010; Shen and Kelleher, 2007; Storandt et al., 2012).

The proteolytic processing of APP that produces Aβ peptides also obligatorily generates the APP intracellular domain (AICD) (Pardossi-Piquard and Checler, 2012). Multiple in vitro and in vivo observations suggest that elevated levels of AICD exert deleterious cell signaling effects (Ghosal et al., 2009; Konietzko, 2012; Pardossi-Piquard and Checler, 2012; Passer et al., 2000). Increased AICD levels are cytotoxic in vitro (Passer et al., 2000) and alter cell signaling pathways (Leissring et al., 2002; Robinson et al., 2014). β-Secretase processing of APP, the proteolytic mechanism that generates Aβ, also generates increased levels of functional AICD compared with nonamyloidogenic APP processing. (Belyaev et al., 2010; Goodger et al., 2009). This suggests that when Aβ levels are increased AICD levels should also be elevated. Indeed, our group has observed increased AICD in human AD brains (Ghosal et al., 2009), thus raising the possibility that increased AICD levels could also play a role in mediating AD pathogenesis. Transgenic mice selectively overexpressing AICD in forebrain and hippocampal neurons (AICD-Tg mice) recapitulate several AD-like pathological features, including tau hyperphosphorylation, aberrant functioning of the hippocampal trisynaptic circuit, and memory deficits (Ghosal and Pimplikar, 2011; Ghosal et al., 2009, 2010; Ryan and Pimplikar, 2005; Vogt et al., 2011).

The exact mechanism by which AICD causes AD-like pathologies in vivo is currently unknown. AICD is known to bind to many cell

* Corresponding author at: Department of Neurosciences, Lerner Research Institute, The Cleveland Clinic, 9500 Euclid Ave/NC30, Cleveland, OH, USA 44195. Tel.: +1 (216) 445 0538; fax: (216)-444-7927.
E-mail address: margevd@ccf.org (D.R. Margevicius).

0197-4580/$ – see front matter © 2015 Elsevier Inc. All rights reserved.
http://dx.doi.org/10.1016/j.neurobiolaging.2015.04.013

signaling proteins (Cao and Sudhof, 2001; Pardossi-Piquard and Checler, 2012; Scheinfeld et al., 2002), including c-Jun N-terminal kinase (JNK)–interacting protein 1 (JIP1) (Matsuda et al., 2001; Scheinfeld et al., 2002), which acts as a scaffold protein for upstream kinases involved in activation of stress-activated protein kinase/JNK (for review, see Davis, 2000). JIP1 is necessary for stress-induced activation of the JNK pathway and its multiple downstream effects (Whitmarsh et al., 2001). Aberrantly-activated JNK is observed in human AD brains (Pei et al., 2001; Yoon et al., 2012; Zhu et al., 2001) and activated JNK has been shown to phosphorylate tau (Orejana et al., 2013; Reynolds et al., 1997), to stimulate the release of proinflammatory cytokines (Arthur and Ley, 2013), to induce cell death (Son et al., 2013), and to modulate neurite outgrowth (Barnat et al., 2010; Oliva et al., 2006). Together, these observations suggest JIP1 may mediate development of AICD-induced AD-like pathologies in AICD-Tg mice. The aim of this study, therefore, is to elucidate if JIP1 is affecting AICD-mediated AD-like effects. To test this hypothesis, we crossed AICD-Tg mice with mice lacking a functional JIP1 gene (Whitmarsh et al., 2001), generating mice that overexpress AICD but lack JIP1 (AICD; JIP1$^{-/-}$) and examined AD-like pathologies, including tau phosphorylation, JNK activation, loss of dendritic spines, and behavioral deficits.

2. Materials and methods

2.1. Mice

AICD-Tg mice are from the FeC$_{\gamma}$25 strain of mice as previously described (Ryan and Pimplikar, 2005). Wild-type (WT) C57BL/6 mice were used as controls. All used mice are on the C57BL/6 background. JIP1$^{-/-}$ mice have been previously generated and characterized (Whitmarsh et al., 2001). To generate AICD; JIP1$^{-/-}$, AICD-Tg mice were mated with mice that were JIP1$^{-/-}$. All mice were aged 8–10 months unless otherwise specified, as advanced tau pathology in AICD-Tg mice is observed at this age (Ghosal et al., 2009). Male and female mice were used. All experiments were approved by the Institutional Animal Care and Use Committee of the Cleveland Clinic.

2.2. Western blotting

Hippocampi from sacrificed mice were dissected away from the cortex and thoroughly homogenized. Ten micrograms of protein (75 μg for AICD Western blotting) was resolved on a 10% Tris-glycine gel (4%–12% NuPAGE gel [Invitrogen] for AICD Western blotting) run at 150 V for 90 minutes (60 minutes for AICD blotting) and transferred to a 0.2-μm nitrocellulose membrane. Antigen retrieval was used for AICD Western blotting as described in Ryan and Pimplikar (2005). Membranes were blocked in blocking solution (5% milk in 1× Tris-buffered saline (TBS) with 0.1% Tween (1× TBS-T), 10% calf serum in 1× TBS-T for AICD Western blots). Primary antibodies used were for AT-8 (1:5000, Thermo Scientific), which recognizes the pSer202/205 site of tau, AT-180 (1:5000, Thermo Scientific), which recognizes the pThr231 site of tau, Tau-5 (1:5000, Invitrogen) which recognizes both phosphorylated and unphosphorylated total tau, p-JNK/SAPK (1:500 Cell Signaling, Santa Cruz, CA, USA), which recognizes pThr183/Tyr185 residues in both the 46 kDa and 54 kDa isoforms of activated JNK, total JNK (1:500 Cell Signaling) which recognizes both phosphorylated and unphosphorylated JNK, APP C-terminal 0443 (1:1000 Calbiochem), and glyceraldehyde-3-phosphate dehydrogenase (1:10,000, Millipore). Secondary antibodies were anti-mouse conjugated to horse radish peroxidase (1:5000; glyceraldehyde-3-phosphate dehydrogenase secondary concentration 1:20,000, Cell Signaling) or anti-rabbit horse radish peroxidase (1:1000 for p-JNK and total JNK Western blots, 1:10,000 for AICD Western blot, Cell Signaling). Bands were visualized using enhanced chemiluminescence developing reagents (Perkin Elmer) and autoradiography film, with exposure times ranging from 10 seconds to 5 minutes (AICD Western blots were exposed 1–20 minutes). Relative densities were assessed using Fiji (ImageJ), with all relevant present bands analyzed simultaneously.

2.3. Immunohistochemistry

Mice were anesthetized with 100 mg/kg of ketamine and 10 mg/kg xylazine mix and transcardially perfused with 1× phosphate-buffered saline (PBS) and 4% paraformaldehyde (PFA) solution in 1× PBS. Brains were postfixed in 4% PFA in PBS and cryoprotected in 30% sucrose solution. Coronal sections (30 μm) were collected using a cryostat. Antigen retrieval was performed for 10 minutes at 95 °C. Sections were exposed to 3% H_2O_2 solution in PBS with 1% Triton-X 100 (1% PBS-T) to abolish any endogenous peroxidase activity. Sections were blocked in 5% goat serum in 0.1% PBS-T solution. The primary antibodies used were AT-8 (1:200, Thermo Scientific), AT-180 (1:200, Thermo Scientific), and p-JNK (1:200, Cell Signaling). Secondary was biotinylated goat anti-mouse antibody (1:200, Vector Laboratories) for AT-8 or AT-180 immunohistochemistry, or goat anti-rabbit (1:200, Vector Laboratories) for p-JNK. Signal was amplified using avidin-biotin complex (1:200, Thermo Scientific). As a control AICD-Tg sections were exposed to only secondary antibody and avidin-biotin complex to discern signal from background staining. Staining was developed using diaminobenzidine. Sections were mounted onto slides and allowed to dry completely. Sections were preserved in xylene and Permount (Fischer Scientific). Sections were imaged using a 20x objective and evaluated for relative intensity of staining. Images from each region were collected and assessed by an investigator blinded to genotype.

2.4. Golgi-Cox staining and imaging

Mice were sacrificed and brains were separated into hemibrains. Hemibrains were then processed for Golgi-Cox staining (FD Rapid GolgiStain Kit; FD NeuroTechnologies). Sagittal sections (50 μm) were obtained using a cryostat. Sections were developed as indicated by the manufacturer, immediately dehydrated, and encased in Permount (Fischer Scientific). Pyramidal neurons in the CA1 were evaluated, as the CA1 is the most drastically affected hippocampal region in human AD patients (Kerchner et al., 2012; La Joie et al., 2013). Four pyramidal neurons were selected randomly and imaged using a 100x objective oil immersion lens. Apical and basal dendrites in pyramidal cells were assessed independently. Three secondary dendrites from the main apical dendrites were selected, as well as 3 basal dendrites 30 μm from the cell body. Images were analyzed using the Fiji software application (ImageJ). Spines were counted along 20 μm of dendrite. The analyzing investigator was blinded to genotype.

2.5. Three-dimensional scanning electron microscopy and reconstruction

Mice were anesthetized and transcardially perfused with 5% glutaraldyhyde and/or 4% PFA solution in Na cacodylate buffer, and a small block of hippocampal tissue (3 × 1 × 1 mm) was stained as described by Ohno et al. (2011). Briefly, tissue was treated with 2% OsO_4 and/or FeCN for 1 hour, followed by 1% thiocarbohydrazide solution for 20 minutes, 2% OsO_4 solution for 30 minutes, an overnight incubation in uranyl acetate solution at 4 °C, and 30 minutes to lead aspartate solution at 60 °C. Samples were dehydrated and embedded in EMbed 812 epoxy resin (Electron Microscopy

Sciences). Samples were mounted and examined in a Zeiss Sigma VP scanning electron microscope equipped with Gatan 3View in-chamber ultramicrotome. Image stacks were assembled and aligned using Fiji (ImageJ) and were analyzed and reconstructed using Reconstruct software (Fiala and Harris, 2001).

2.6. Novel object behavioral analysis

Trials for each mouse lasted 10 minutes and were completed in 3 consecutive days. On the first day mice were placed in the testing chamber (60 × 50 × 40 cm dimensions). On the second day, 2 identical objects were placed in the chamber. On the third day, 1 of the objects was replaced with a novel object. Video was taken of each trial. The analyzing investigator, blinded to genotype, manually assessed time spent exploring objects. Any mouse exhibiting a total exploration time of <5 seconds was blindly excluded from analysis. The chamber was cleaned with 70% ethanol after each trial.

2.7. Fear conditioning behavioral analysis

The used protocol was adopted from Ponder et al. (2008). Briefly, mice were placed in a chamber for 5 minutes, with 3 minutes of chamber exploration, with subsequent exposure twice to a 20-second tone followed by a 2-second shock of 0.5 mV, with an interval of 15 seconds between each tone and shock. The second day of the protocol was eliminated, as we have observed that AICD-Tg mice do not exhibit deficits in contextual fear-related memory (unpublished data). Two days after initial exposure to the chamber, the walls and floor of the chamber were altered. The mouse was then exposed to the sound stimulus without the subsequent shock. Freezing behavior associated with the stimulus was assessed using the FreezeView software package. The chamber was cleaned with 70% ethanol after each trial.

2.8. Statistical analysis

All statistical analysis was done using Prism software (version 5). All data was assessed using 1-way analyses of variance to determine statistical significance, with $p < 0.05$ defined as significant. Error bars in each case represent standard error of the mean.

3. Results

3.1. AICD; JIP1$^{-/-}$ mice showed decreased phospho-tau levels compared with AICD-Tg mice

AICD-Tg mice start to show elevated phospho-tau levels, as assessed by both AT-8 and AT-180 antibodies, by 4 months of age (Ghosal et al., 2009), and a number of protein kinases, including JNK, have been implicated in tau phosphorylation (Johnson and Stoothoff, 2004; Reynolds et al., 1997). JIP1's known effects on JNK signaling, therefore, could affect tau pathology observed in AICD-Tg mice. To determine whether the absence of JIP1 affects phospho-tau levels in AICD-Tg mice, WT, AICD-Tg, and AICD; JIP1$^{-/-}$ mice were sacrificed and brain sections were analyzed by immunohistochemistry using the AT-8 anti–phospho-tau antibody. As shown previously, AICD-Tg mice exhibit increased levels of phospho-tau in neurons in the hilus of the dentate gyrus and the CA3 region of the hippocampus compared with WT brains (Fig. 1A). Increased staining was observed throughout all brain regions in AICD-Tg mice, including the CA1 of the hippocampus, but was less pronounced in other regions. By contrast, AICD; JIP1$^{-/-}$ mice displayed dramatically reduced phospho-tau staining in each of these regions (Fig. 1A), and often levels of phospho-tau were observed to be below those in WT animals. Similarly, brain sections stained with the AT-180 phospho-tau antibody also showed increased phospho-tau levels in AICD-Tg mice, which were reduced in AICD; JIP1$^{-/-}$ mice (Fig. 1B). These data show that loss of JIP1 protects AICD-Tg mice from increasing tau phosphorylation.

To further corroborate these observations and to obtain semi-quantitative data, brain tissue was analyzed by Western blotting using AT-8 and AT-180 antibodies. Western blotting confirmed that levels of phosphorylated tau are reduced in AICD; JIP1$^{-/-}$ mice compared with AICD-Tg mice, suggesting normal levels of phosphorylated tau are observed in AICD; JIP1$^{-/-}$ (Fig. 1C–E). Total tau levels were unaffected between genotypes (Fig. 1F).

3.2. Decreased phospho-JNK levels are observed in AICD; JIP1$^{-/-}$ mice compared with AICD-Tg mice

JNK is known to be activated in clinical AD and thus may affect AD pathogenesis (Pei et al., 2001; Yoon et al., 2012; Zhu et al., 2001). Ordinarily basal levels of JNK activation are unaffected in JIP1$^{-/-}$ mice, with JIP1 specifically mediating stress-specific JNK signaling (Whitmarsh et al., 2001). To determine if increased AICD-JIP1 interaction facilitates increased activation of the JNK pathway levels of activated, phosphorylated JNK were assessed in WT, AICD-Tg, and AICD; JIP1$^{-/-}$ mice by Western blot. Whereas WT mice showed basal levels of phospho-JNK (Fig. 2A, lanes 1–3), phospho-JNK levels were elevated in AICD-Tg mice (lanes 4–6), but were decreased in AICD; JIP1$^{-/-}$ mice compared with levels observed in AICD-Tg mice (lanes 7–9). However, due to high variability in phospho-JNK levels between all groups, the differences were not statistically significant (Fig. 2B) [When groups were compared by paired *t* test p-JNK was significantly decreased in AICD; JIP1$^{-/-}$ mice compared with AICD-Tg mice, $p = 0.0416$. All other *t* test comparisons were not significant]. These data suggest that there is a tendency for AICD-Tg mice to exhibit elevated levels of phospho-JNK, which are decreased in the absence of JIP1. Levels of total JNK were similar between all genotypes (Fig. 2C). To further confirm JNK is increasingly activated in AICD-Tg mice, we performed immunohistochemistry for phosphorylated JNK. We observed an increase in phospho-JNK staining in AICD-Tg mice compared with both WT and AICD; JIP1$^{-/-}$ mice (Supplementary Fig. 1). Interestingly, the regions with the strongest difference in p-JNK immunoreactivity are also regions that stained strongly for phosphorylated tau, namely the dentate gyrus and the CA3 region of the hippocampus. This further suggests AICD-Tg mice exhibit increased JNK activation through increased AICD-JIP1 interaction, and that this interaction facilitates and potentiates development of tau pathology.

3.3. Relative AICD levels are increased in AICD; JIP1$^{-/-}$ mice despite lack of JIP1

AICD is known to bind many cytosolic proteins, some of which serve a role in stabilizing AICD (Cao and Sudhof, 2001; Pardossi-Piquard and Checler, 2012; Scheinfeld et al., 2002). It is unknown if JIP1 serves a role in stabilizing AICD. However, JIP1 primarily serves to mediate cell signaling rather than stabilize proteins. Therefore, we hypothesized that increased AICD levels are persistently observed in AICD; JIP1$^{-/-}$ mice, and that lack of JIP1 mediates changes in cell signaling rather than overall AICD levels. To test this hypothesis, we performed a Western blot for levels of AICD in WT, AICD-Tg, and AICD; JIP1$^{-/-}$ mice using an antibody for the APP C-terminus using a protocol previously described (Ryan and Pimplikar, 2005). We found AICD-Tg mice (Fig. 3A, lanes 3–5), as expected, exhibit increased levels of AICD compared with WT mice (Fig. 3A, lanes 1–2). We also found that AICD; JIP1$^{-/-}$ mice (Fig. 3A, lanes 6–9) exhibit increased levels of AICD to compared with WT

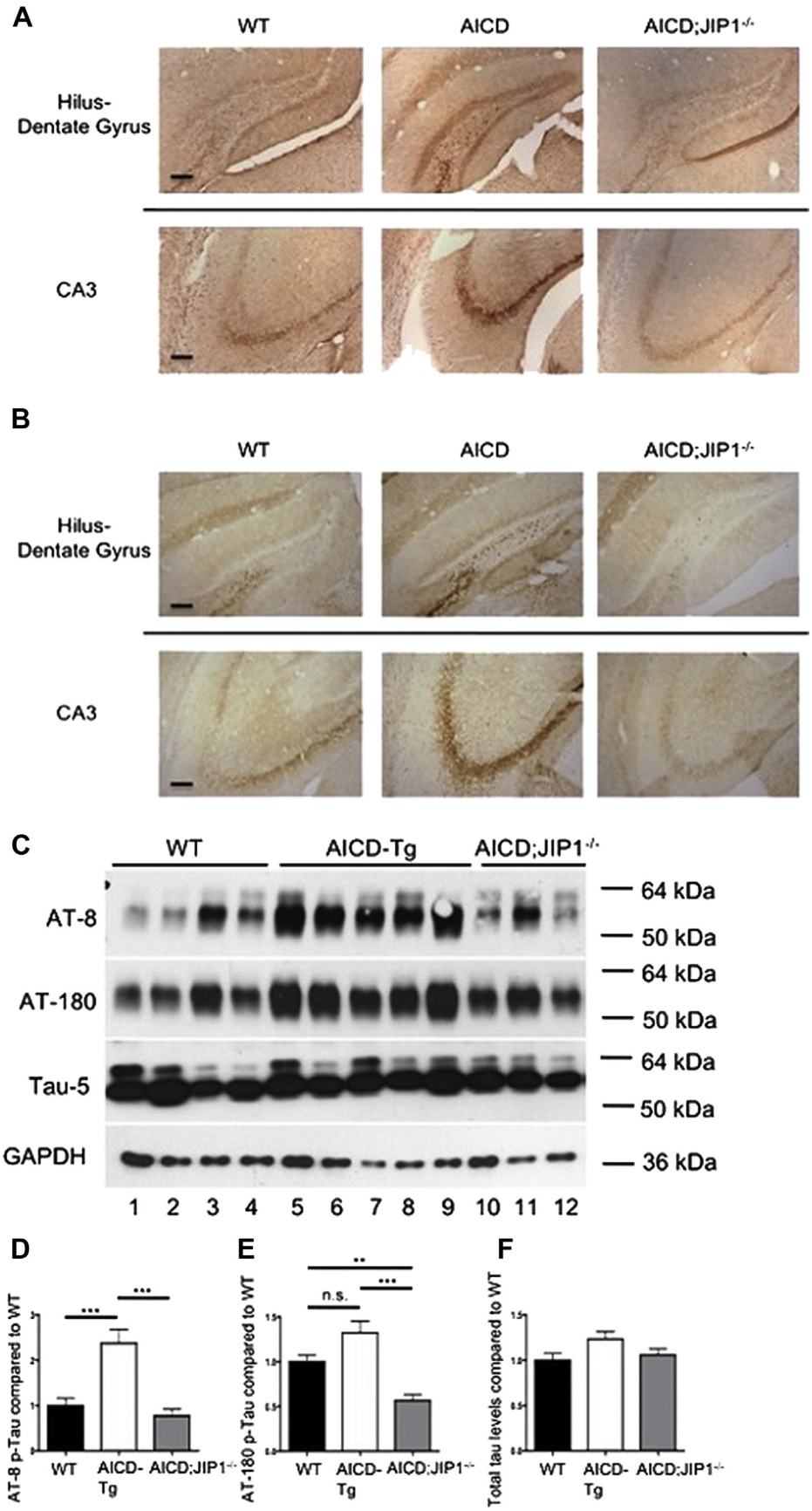

Fig. 1. Decreased phospho-tau levels are observed in AICD; JIP1$^{-/-}$ mice. (A) Distribution of phospho-tau in the hilus of the dentate gyrus and CA3 regions of the hippocampus as detected by AT-8 immunostaining. AT-8 demonstrates some cell-specific staining in the hippocampus in wild-type (WT) mice, an increased cell-specific staining in the dentate gyrus

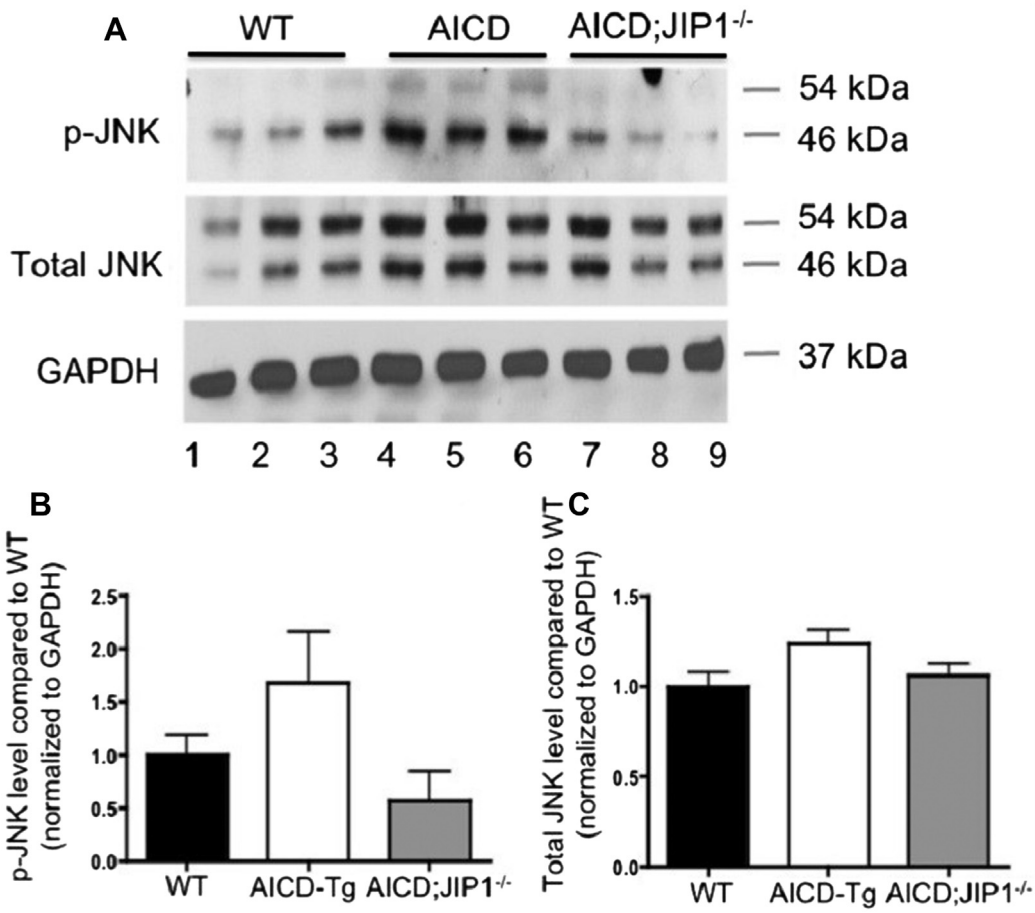

Fig. 2. JNK signaling was decreased in AICD; JIP1$^{-/-}$ mice. (A) Western blot assessing JNK activation in hippocampal protein lysates from wild-type (WT) (lanes 1–3), AICD-Tg (lanes 4–6), and AICD; JIP1$^{-/-}$ (lanes 7–9) mice. Lysates were assessed for levels of phospho-JNK (p-JNK) and total JNK. (B) Graph quantifying levels of p-JNK. A trend is observed indicating increased levels of p-JNK in AICD-Tg mice compared with WT and AICD; JIP1$^{-/-}$ mice, but increased variability between animals indicates this increase is not significant by 1-way analysis of variance (ANOVA). However, the trend and individual *t* test comparisons suggest basal levels of p-JNK are observed in AICD; JIP1$^{-/-}$ mice. (C) Total JNK levels were unchanged between genotypes, suggesting effects were observed on p-JNK levels specifically. Data were analyzed using ANOVA with Tukey's post hoc test to assess individual significances between groups, and individual unpaired *t* tests between each group. n ≥ 6 animals for each genotype. Abbreviations: AICD, amyloid precursor protein intracellular domain; GAPDH, glyceraldehyde-3-phosphate dehydrogenase; JIP1, c-Jun N-terminal kinase–interacting protein 1; JNK, c-Jun N-terminal kinase, p-JNK, phosphorylated c-Jun N-terminal kinase; Tg, transgenic.

mice, comparable to levels in AICD-Tg mice (Fig. 1A). Quantification of this data suggests AICD-Tg and AICD; JIP1$^{-/-}$ mice exhibit AICD levels 22.9% and 17.6% greater than WT levels, respectively (Fig. 3B). This evidence suggests JIP1 does not stabilize AICD, and that AICD; JIP1$^{-/-}$ mice are protected from development of AD-like pathologies through lack of the AICD-JIP1 interaction.

3.4. AICD; JIP1$^{-/-}$ mice do not exhibit spine deficits present in AICD-Tg mice

Studies in various mouse models of AD have demonstrated that the increasing presence of hyperphosphorylated tau can cause tau aggregation that mediates loss of dendritic spines (Chabrier et al., 2014; Kopeikina et al., 2013a, 2013b; Zempel et al., 2010). Therefore, we assessed AICD-Tg mice for dendritic spine deficits and whether those deficits were rescued in AICD; JIP1$^{-/-}$ mice. Dendritic spine density was evaluated by performing Golgi-Cox staining on hemibrains from 3-, 12-, and 18-month-old mice. Hemibrains were sectioned, and the CA1 region of the hippocampus was examined. No deficit in dendritic spine density was observed in AICD-Tg mice at 3 months of age compared with WT. AICD; JIP1$^{-/-}$ mice also exhibit a spine density comparable to WT mice (Fig. 4A). However, 12-month-old AICD-Tg mice demonstrated a decreased spine number compared with age-matched WT mice

in AICD-Tg mice, and staining similar to WT in AICD; JIP1$^{-/-}$ mice. (B) AT-180 also shows increased immunoreactivity in AICD-Tg mice, whereas AICD; JIP1$^{-/-}$ mice exhibit levels of tau phosphorylation comparable to WT mice. Scale bar represents 25 μm, n = 3 animals for each genotype. At least 4 hippocampal sections per animal were visualized. (C) Representative Western blot assessing levels of phosphorylated tau (phospho-tau) in hippocampal protein lysates from WT (lanes 1–4), AICD-Tg (lanes 5–9), and AICD; JIP1$^{-/-}$ (lanes 10–12) mice. Lysates were assessed for levels of phospho-tau at different epitopes (AT-8 and AT-180). Total levels of tau were assessed using the Tau-5 antibody. (D and E) (D) AICD-Tg mice exhibit increased levels of AT-8 phospho-tau compared with WT. (E) There is no significant difference between WT and AICD-Tg mice detected by AT-180, but the trend coupled with the immunohistochemistry data suggests increased tau phosphorylation is observed in AICD-Tg mice. (D and E) AICD; JIP1$^{-/-}$ mice exhibit less phospho-tau both at AT-8 and AT-180 compared with AICD-Tg mice, suggesting lessened tau pathology. Interestingly, AICD; JIP1$^{-/-}$ mice demonstrate decreased levels of AT-180 compared with WT. (F) Total tau levels were not significantly different between genotypes. Data were analyzed using analysis of variance with Tukey's post hoc test to assess individual significances between groups. n ≥ 6 animals for each genotype $^{**}p < 0.01$ and $^{***}p < 0.001$. Abbreviations: AICD, amyloid precursor protein intracellular domain; GAPDH, glyceraldehyde-3-phosphate dehydrogenase; JIP1, c-Jun N-terminal kinase–interacting protein 1; Tg, transgenic.

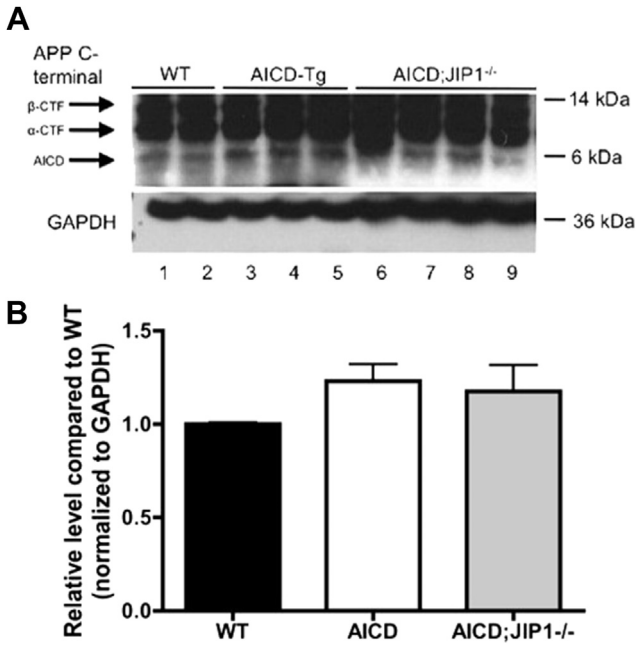

Fig. 3. AICD levels remain increased in AICD; J IP1$^{-/-}$ mice despite lack of JIP1. (A) AICD levels were assessed using Western blotting from hippocampal protein lysates from wild-type (WT) (lanes 1–2), AICD-Tg (lanes 3–5), and AICD; JIP1$^{-/-}$ (lanes 6–9) mice. AICD levels were observed to be increased in AICD-Tg mice compared with WT mice. AICD; JIP1$^{-/-}$ mice also exhibit increased AICD levels compared with WT mice, and exhibit levels comparable to what is observed in AICD-Tg mice. (B) Quantification of AICD blots. AICD levels are elevated in AICD-Tg and AICD; JIP1$^{-/-}$ mice compared with WT. n ≥ 3 animals for each genotype. Abbreviations: βCTF, beta C-terminal fragment, αCTF, alpha C-terminal fragment, AICD, amyloid precursor protein intracellular domain, APP, amyloid precursor protein; GAPDH, glyceraldehyde-3-phosphate dehydrogenase; JIP1, c-Jun N-terminal kinase–interacting protein 1.

and AICD; JIP1$^{-/-}$ mice (Fig. 4B). This phenomenon was also present in 18-month-old mice (Fig. 4C). Quantification of these data showed a deficit in dendritic spine density in AICD-Tg compared with WT or AICD; JIP1$^{-/-}$ mice (Fig. 4D). Spine density was also measured in the basal dendrites in 12-month-old mice and was observed as reduced in AICD-Tg mice. However, these deficits were not observed to be persistent at 18 months (data not shown). To further confirm this observation, we visualized apical dendrites from mice aged 18 months and spines that connect to the dendrite using serialized scanning electron microscopy (Fig. 4E). After identifying these structures through the stack of micrographs we then extracted that data and performed a 3-dimensional reconstruction of the dendrite. We found that AICD-Tg mice exhibit fewer spines than any of the other genotypes analyzed, confirming our previous observations from Golgi staining (Fig. 4F).

3.5. Functional preservation of recognition memory and cued fear conditioning was observed in AICD; JIP1$^{-/-}$ mice

Because lack of JIP1 in AICD-Tg mice prevented deficits in dendritic spine density, which are directly associated with loss of excitatory synaptic function, we investigated whether it also prevented functional memory deficits in AICD-Tg mice. Mice were subjected to 2 behavior tests to examine different aspects of neural function related to memory: novel object testing to test hippocampal recognition memory and classical fear conditioning to test fear-related memory associated with more global neurologic function. In novel object testing mice that exhibit a preference for exploring the novel object exhibit a retained ability to recognize the familiar object, associated with intact recognition memory. WT mice exhibited a preference for the novel object in novel object recognition testing, whereas AICD-Tg mice showed no preference between objects, indicating AICD-Tg mice experience a loss of recognition memory (Fig. 5A). Interestingly, AICD ; JIP1$^{-/-}$ mice retained the ability to discriminate between the novel and familiar object. As expected, JIP1$^{-/-}$ behaved similar to WT mice. Similarly, AICD-Tg mice showed deficits in freezing behavior associated with classical fear conditioning (Fig. 5B) as compared with WT mice, and this deficit was also alleviated in AICD; JIP1$^{-/-}$ mice. AICD-Tg mice showed no deficits in an open field test compared with WT mice (Ghosal et al., 2009), suggesting that differences in these tests were due to memory deficits and not general motor impairments.

4. Discussion

The major finding of the present study is that in AICD-Tg mice JIP1 is required for the development of AD-like pathological features and memory impairments, and lack of JIP1 protects AICD-Tg mice from tau hyperphosphorylation, increased JNK activation, loss of dendritic spines, and behavioral deficits. Recent findings that 20%–30% of clinically diagnosed AD patients do not show amyloid deposits by positron emission tomographic imaging (Jack et al., 2012; Knopman et al., 2012, 2013) further strengthens the notion that amyloid-independent mechanisms are also strongly operative in AD. This evidence further suggests the value of the AICD-Tg mouse model to study amyloid-independent cellular mechanisms of AD pathogenesis.

4.1. JNK activation in AD

These results show that JIP1 can affect the deleterious effects of AICD. Previous studies have shown that JIP1-b, a neuronally-expressed, alternatively-spliced product of ubiquitously expressed JIP1, binds the AICD portion of APP-CTF (Matsuda et al., 2001; Scheinfeld et al., 2002). JIP1 is a cytoplasmic scaffold protein that binds JNK and its upstream activating kinases, mitogen-activated protein kinase kinase 4 and mixed lineage kinase 7, to facilitate activation of the JNK pathway in response to cellular stress (Davis, 2000). A number of studies have shown that JNK is abnormally activated in the brains of AD patients (Pei et al., 2001; Shoji et al., 2000; Yoon et al., 2012; Zhu et al., 2001). Previous studies have shown that intracellular Aβ or oligomeric Aβ can also trigger JNK activation (Shoji et al., 2000; Yoon et al., 2012). Because AICD-Tg mice show normal levels of Aβ (Ghosal et al., 2009), the present data suggest that AICD can also activate the JNK pathway via JIP1 and thus contribute to AD pathogenesis independently from Aβ. JNK is known to phosphorylate tau (Orejana et al., 2013; Reynolds et al., 1997), and JIP1 has been shown to directly interact with tau (Ittner et al., 2009), raising the possibility that JIP1 facilitates increased tau phosphorylation by promoting proximity of activated JNK to tau. Although AICD is known the bind the phosphotyrosine-binding domain of JIP1-b via its 'YENPTY' motif, further studies are needed to understand how this interaction activates the JNK cascade, as the exact mechanism by which these mice develop pathology needs further elaboration.

The FeCγ25 AICD-Tg model, our group has previously described (Ghosal and Pimplikar, 2011; Ghosal et al., 2010, 2009; Ryan and Pimplikar, 2005; Vogt et al., 2011) is unique in that it also over-expresses Fe65, which stabilizes the AICD. This model also exhibits increased cytoplasmic presence of AICD (Ryan and Pimplikar, 2005). JIP1 is known to be primarily located in the cytoplasm, only experiencing perinuclear localization in response to stress activation (Whitmarsh et al., 2001) and is normally localized primarily to the termini of axons (Dajas-Bailador et al., 2008). Therefore, the enhanced cytoplasmic presence of AICD in our model brings it in closer proximity to JIP1 and thus may be the key to how

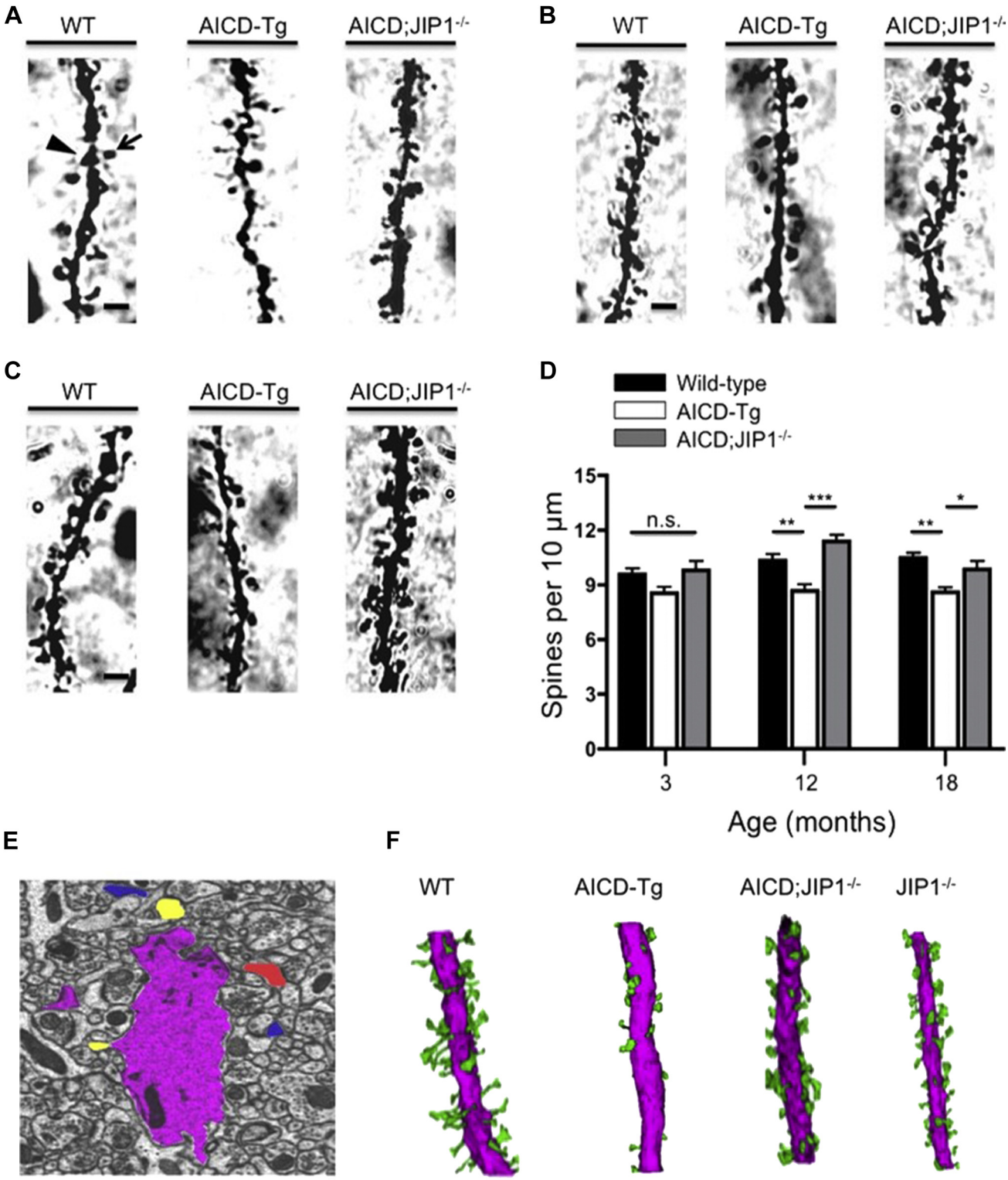

Fig. 4. Spine density deficits not present in AICD; JIP1$^{-/-}$ mice. Mice were of the age indicated. (A) Representative apical dendrites from 3-month-old mice. No significant difference is observed between genotypes. The open arrow indicates what is considered a dendritic spine due to its characteristic structure. The closed arrowhead indicates an uncharacteristic structure that was not considered to be a spine. (B) Representative apical dendrites from mice aged 12 months. AICD-Tg mice exhibit fewer spines. (C) Representative apical dendrites from mice 18 months of age. AICD-Tg mice exhibit a persistent spine deficit as they age, and AICD; JIP1$^{-/-}$ mice also demonstrate a spine density similar to what is observed in WT mice. All scale bars represent 2.5 µm. (D) Quantification of apical spine density in relevant genotypes at 3, 12, and 18 months of age. Spine deficits are not observed at 3 months, indicating deficits are age-dependent. WT mean = 9.58 spines per 10 µm ± 2.7, AICD-Tg mean = 8.55 ± 2.7, AICD; JIP1$^{-/-}$ mean = 9.82 ± 2.96. Spine deficits are first observed at 12 months of age in AICD-Tg mice. AICD; JIP1$^{-/-}$ mice demonstrate spine densities comparable to WT mice. WT mean = 10.33 spines per 10 µm ± 2.8, AICD-Tg mean = 8.67 ± 2.9, AICD; JIP1$^{-/-}$ mean = 11.38 ± 2.08. Deficits are persistent at 18 months of age, which are also absent in AICD; JIP1$^{-/-}$ mice. WT mean = 10.48 spines per 10 µm ± 1.77, AICD-Tg mean = 8.58 ± 2.67, AICD; JIP1$^{-/-}$ mean = 9.87 ± 2.62. Differences were assessed in apical dendrites using analysis of variance with Tukey's post hoc test for differences between groups. n ≥ 36, 3 dendrites per neuron, 4 neurons per animal, ≥3 animals assessed for each genotype $^{*}p < 0.05$, $^{**}p < 0.01$ $^{***}p < 0.001$. (E) Representative electron micrograph of a dendrite from the CA1 region of the hippocampus. Dendrites were identified and colored in using computer software to in order to perform

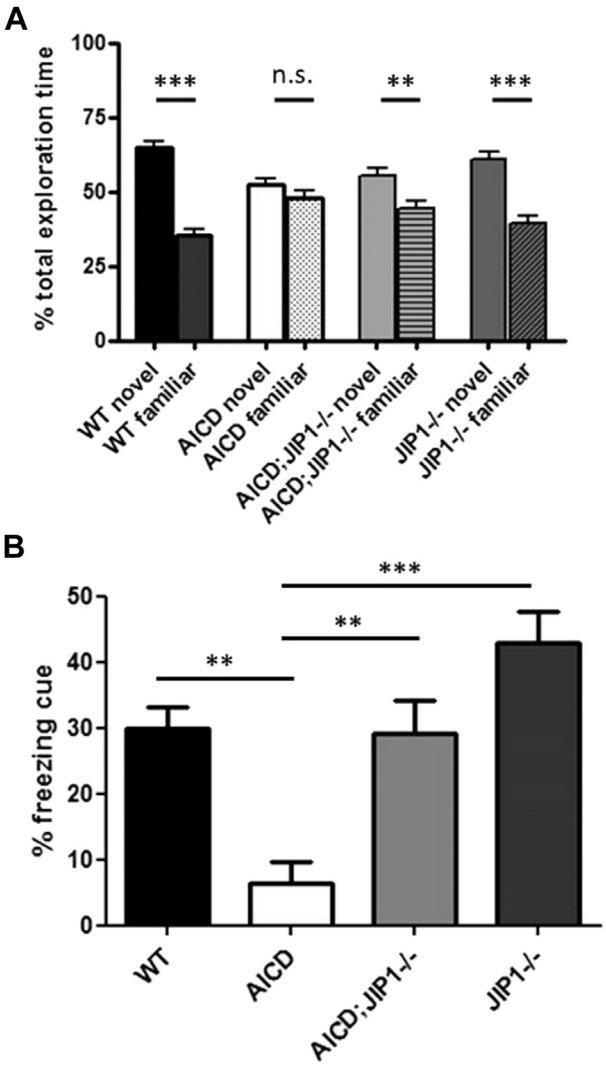

Fig. 5. Recognition and fear-associated-memory is intact in AICD; JIP1$^{-/-}$ mice. (A) In novel object behavioral testing, AICD-Tg mice exhibited a lack of preference for the novel object, demonstrating a deficit in hippocampal recognition memory. Age-matched AICD; JIP1$^{-/-}$ mice retain preference for the novel object, demonstrating intact recognition memory. JIP1$^{-/-}$ mice also demonstrate intact recognition memory. Data were analyzed using analysis of variance (ANOVA) with Bonferroni's correction to compare selected groups to demonstrate significant preference within each genotype only. n $\geq$ 8 animals for each genotype $^{**}p < 0.01$ and $^{***}p < 0.001$. (B) Mice were assessed using classical fear conditioning for deficits in fear-based memory. AICD-Tg mice exhibit a deficit in freezing behavior associated with cued fear memory, whereas AICD; JIP1$^{-/-}$ mice exhibit fear memory comparable to WT mice. Data were analyzed using ANOVA with Tukey's post hoc test for differences between groups n $\geq$ 8 animals for each genotype $^{**}p < 0.01$ and $^{***}p < 001$. Abbreviations: AICD, amyloid precursor protein intracellular domain; JIP1, c-Jun N-terminal kinase–interacting protein 1; Tg, transgenic; WT, wild type.

a phenotype develops in FeCγ25 AICD-Tg mice. This may also somewhat explain why other groups that have generated AICD-overexpressing mice do not observe a phenotype (Giliberto et al., 2010), as increased levels of cytoplasmic AICD caused by Fe65 stabilization may mediate AD-like pathogenesis in FeCγ25 AICD-Tg mice, which would allow AICD to complex more readily with its other cytoplasmic-interacting proteins, such as JIP1. This suggests AICD may be facilitating a cytoplasmic signaling role of JIP1. However, a facilitated role for JIP1-related nuclear signaling cannot be excluded, as JIP1 is shown to affect transcriptional activity, as well, in a manner analogous to, yet independent from, Fe65 (Konietzko et al., 2010; Scheinfeld et al., 2003). This work also further suggests increased AICD presence, rather than the AICD-Fe65 complex, is affecting pathology in our mice, as Fe65 and JIP1 bind AICD at the same site indicating they likely bind AICD separately and thus have separate cell signaling effects (Cao and Sudhof, 2001; Matsuda et al., 2001).

4.2. Loss of synapses in AD

An interesting finding of our study is that, in AICD-Tg mice, loss of dendritic spines, which is indicative of loss of excitatory synapses, is alleviated in the absence of JIP1. Synaptic loss is the most critical pathological feature of AD and is best correlated with disease progression (Selkoe, 2002; Terry et al., 1991). The likely causes underlying the observed spine deficits is spine loss associated with increased aggregation and mislocalization of tau into dendrites. Indeed, spine loss associated with tau mislocalization and aggregation is observed in other mouse models that exhibit tau pathology (Chabrier et al., 2014; Hoover et al., 2010; Kopeikina et al., 2013a, 2013b). Specifically, tau aggregation is likely contributing to spine loss in AICD-Tg mice because we do not see spine loss with increased phospho-tau at 3–4 months of age, but see spine loss after 8–9 months of age, when tau increasingly aggregates in our mouse model (Ghosal et al., 2009). The mechanistic details regarding how tau mislocalization and aggregation causes spine loss, however, are not yet fully understood.

An interesting observation is that age-dependent loss of dendritic spines in AICD-Tg mice is because of an increase in spine number in WT and AICD; JIP1$^{-/-}$ mice instead of a real decrease in AICD-Tg mice. As increasing tau phosphorylation mediates spine loss rather than causing failure of spine development in other mouse models of tau dysfunction, and as AICD-Tg mice develop pathology in an age-dependent manner (Ghosal et al., 2009) we believe AICD-Tg mice are losing spines as they age rather than failing to develop spines. Tau mislocalization renders microtubules unstable and destabilizes presynaptic termini that synapse with dendritic spines, which can result in spine loss (Bendiske et al., 2002; Erez et al., 2014; Harris et al., 2012). Aggregated tau may also be exhibiting a toxic gain-of-function effect, causing synaptic dysfunction in the postsynaptic dendrites where it is mislocalized (Chabrier et al., 2014). There is in vitro evidence showing that tau mediates the spine loss induced by Aβ and in vivo evidence that both pathologies can synergistically contribute to spine loss (Chabrier et al., 2014; Zempel et al., 2010). This evidence suggests it is likely both amyloid-dependent and amyloid-independent mechanisms of spine loss are mediated primarily by tau and that both Aβ and tau contribute synergistically to synaptic loss in clinical AD.

a 3-dimensional reconstruction by extracting information through coloration from serialized scanning electron micrographs in sequence. Active spines were identified by presence of both a presynaptic terminal and a postsynaptic density. Magenta structure is the dendritic shaft, multicolored structures are spines identified to link to the dendritic shaft innervated by a presynaptic density (indicated by the presence of synaptic vesicles in the innervating terminus) and a postsynaptic density (dark, dense structure between the synapse) (F) Representative 3D reconstructions of each genotype from mice aged 18 months. AICD-Tg mice exhibit fewer spines than WT, AICD; JIP1$^{-/-}$, or JIP1$^{-/-}$ mice, further establishing AICD-Tg mice experience deficits in spine density. Purple structure is the dendritic shaft, green structures are functional innervated dendritic spines. n = 18, 6 dendrites per mouse, 3 mice for WT and AICD-Tg mice, n = 6, 6 dendrites per mouse, 1 mouse for AICD; JIP1$^{-/-}$ and JIP1$^{-/-}$. Abbreviations: AICD, amyloid precursor protein intracellular domain; JIP1, c-Jun N-terminal kinase–interacting protein 1; Tg, transgenic; WT, wild type. (For interpretation of the references to color in this figure legend, the reader is referred to the Web version of this article.)

An important finding of the present study is that loss of JIP1 not only protected AICD-Tg mice from developing AD-histopathologies but also protected mice from behavioral deficits in 2 behavioral tests that depend on different brain functions. By 8 months of age, AICD-Tg mice became deficient in both novel object and classical fear conditioning tests, showing that both hippocampal and more global neurologic function was compromised. JIP1, therefore, mediates not only the histopathological features induced by AICD but also mediates its neurological effects. JIP1$^{-/-}$ mice were not behaviorally impaired in these tests, indicating that JIP1 function is not required for normal memory function. This is consistent with previous in vivo observations, as although in vitro observations indicate lack of JIP1 can mediate N-methyl-d-aspartate receptor dysfunction (Kennedy et al., 2007) in vivo lack of JIP1 results in a neurologically normal phenotype (Whitmarsh et al., 2001).

4.3. The role of AICD in human AD

Studies indicating increased levels of functional AICD are released by β-secretase (Belyaev et al., 2010; Goodger et al., 2009) offer evidence that increased AICD levels are expected to occur concomitantly with increased Aβ, offering an explanation for why increased AICD levels are observed in human AD (Ghosal et al., 2009). This work shows that AICD may contribute to AD pathogenesis independent of Aβ through activation of the JNK pathway. Thus, although the causative role of AICD in AD remains to be established, available data indicate that AICD could be an important candidate for amyloid-independent mechanisms of AD pathogenesis. The JNK signaling pathway is known to activate activator protein-1 and nuclear factor kappa b signaling, which dramatically affect innate immune pathways (Arthur and Ley, 2013). Recently, evidence from genome-wide association studies, and systems biology studies have strongly implicated innate immunity in the onset of clinical AD (Jones et al., 2010; Zhang et al., 2013). Therefore, AICD may contribute significantly to clinical AD by increasing innate immune signaling activation through increasing JNK pathway activation by its effects on JIP1. Our findings also suggest a possible explanation as to why the removal of Aβ peptides alone may not be sufficient to block the progression of disease and suggest that a combination therapy involving multiple targets may be more effective than monotherapy focused exclusively on Aβ.

Disclosure statement

None of the authors have any actual or potential financial or personal conflicts of interest to declare.

Acknowledgements

This work was funded by a grant from the Alzheimer's Association, and by Kleasens Family Philanthropic Funds to SWP. The authors would like to thank Grahame Kidd for his critical insights and help with both the Golgi-Cox imaging and 3D electron microscopy, Shane Bemiller for his help with Western blotting protocols, and Drs. Bruce Lamb, Chris Nelson, Kaushik Ghosal, and Ms. Lana Pollock for their comments and suggestions on the manuscript. None of these sources were directly involved in design of the study, or in the collection, analysis, and interpretation of the data, or in the decision to write or submit this report.

Appendix A. Supplementary data

Supplementary data associated with this article can be found, in the online version, at http://dx.doi.org/10.1016/j.neurobiolaging.2015.04.013.

References

Arthur, J.S., Ley, S.C., 2013. Mitogen-activated protein kinases in innate immunity. Nat. Rev. Immunol. 13, 679–692.
Barnat, M., Enslen, H., Propst, F., Davis, R.J., Soares, S., Nothias, F., 2010. Distinct roles of c-Jun N-terminal kinase isoforms in neurite initiation and elongation during axonal regeneration. J. Neurosci. 30, 7804–7816.
Belyaev, N.D., Kellett, K.A., Beckett, C., Makova, N.Z., Revett, T.J., Nalivaeva, N.N., Hooper, N.M., Turner, A.J., 2010. The transcriptionally active amyloid precursor protein (APP) intracellular domain is preferentially produced from the 695 isoform of APP in a -secretase-dependent pathway. J. Biol. Chem. 285, 41443–41454.
Bendiske, J., Caba, E., Brown, Q.B., Bahr, B.A., 2002. Intracellular deposition, microtubule destabilization, and transport failure: an "early" pathogenic cascade leading to synaptic decline. J. Neuropathol. Exp. Neurol. 61, 640–650.
Cao, X., Sudhof, T.C., 2001. A transcriptionally [correction of transcriptively] active complex of APP with Fe65 and histone acetyltransferase Tip60. Science 293, 115–120.
Chabrier, M.A., Cheng, D., Castello, N.A., Green, K.N., Laferla, F.M., 2014. Synergistic effects of amyloid-beta and wild-type human tau on dendritic spine loss in a floxed double transgenic model of Alzheimer's disease. Neurobiol. Dis. 64, 107–117.
Dajas-Bailador, F., Jones, E.V., Whitmarsh, A.J., 2008. The JIP1 scaffold protein regulates axonal development in cortical neurons. Curr. Biol. 18, 221–226.
Davis, R.J., 2000. Signal transduction by the JNK group of MAP kinases. Cell 103, 239–252.
Erez, H., Shemesh, O.A., Spira, M.E., 2014. Rescue of tau-induced synaptic transmission pathology by paclitaxel. Front. Cell. Neurosci. 8, 34.
Fiala, J.C., Harris, K.M., 2001. Extending unbiased stereology of brain ultrastructure to three-dimensional volumes. J. Am. Med. Inform. Assoc. 8, 1–16.
Ghosal, K., Pimplikar, S.W., 2011. Aging and excitotoxic stress exacerbate neural circuit reorganization in amyloid precursor protein intracellular domain transgenic mice. Neurobiol. Aging 32, 2320.e1–2320.e9.
Ghosal, K., Stathopoulos, A., Pimplikar, S.W., 2010. APP intracellular domain impairs adult neurogenesis in transgenic mice by inducing neuroinflammation. PLoS One 5, e11866.
Ghosal, K., Vogt, D.L., Liang, M., Shen, Y., Lamb, B.T., Pimplikar, S.W., 2009. Alzheimer's disease-like pathological features in transgenic mice expressing the APP intracellular domain. Proc. Natl. Acad. Sci. U. S. A. 106, 18367–18372.
Giliberto, L., d'Abramo, C., Acker, C.M., Davies, P., D'Adamio, L., 2010. Transgenic expression of the amyloid-beta precursor protein-intracellular domain does not induce Alzheimer's disease-like traits in vivo. PLoS One 5, e11609.
Goate, A., Hardy, J., 2012. Twenty years of Alzheimer's disease-causing mutations. J. Neurochem. 120 (Suppl 1), 3–8.
Goodger, Z.V., Rajendran, L., Trutzel, A., Kohli, B.M., Nitsch, R.M., Konietzko, U., 2009. Nuclear signaling by the APP intracellular domain occurs predominantly through the amyloidogenic processing pathway. J. Cell Sci. 122 (Pt 20), 3703–3714.
Hardy, J., Selkoe, D.J., 2002. The amyloid hypothesis of Alzheimer's disease: progress and problems on the road to therapeutics. Science 297, 353–356.
Harris, J.A., Koyama, A., Maeda, S., Ho, K., Devidze, N., Dubal, D.B., Yu, G.Q., Masliah, E., Mucke, L., 2012. Human P301L-mutant tau expression in mouse entorhinal-hippocampal network causes tau aggregation and presynaptic pathology but no cognitive deficits. PLoS One 7, e45881.
Hoover, B.R., Reed, M.N., Su, J., Penrod, R.D., Kotilinek, L.A., Grant, M.K., Pitstick, R., Carlson, G.A., Lanier, L.M., Yuan, L.L., Ashe, K.H., Liao, D., 2010. Tau mislocalization to dendritic spines mediates synaptic dysfunction independently of neurodegeneration. Neuron 68, 1067–1081.
Ittner, L.M., Ke, Y.D., Gotz, J., 2009. Phosphorylated Tau interacts with c-Jun N-terminal kinase-interacting protein 1 (JIP1) in Alzheimer disease. J. Biol. Chem. 284, 20909–20916.
Jack Jr., C.R., Knopman, D.S., Weigand, S.D., Wiste, H.J., Vemuri, P., Lowe, V., Kantarci, K., Gunter, J.L., Senjem, M.L., Ivnik, R.J., Roberts, R.O., Rocca, W.A., Boeve, B.F., Petersen, R.C., 2012. An operational approach to National Institute on Aging-Alzheimer's Association criteria for preclinical Alzheimer disease. Ann. Neurol. 71, 765–775.
Johnson, G.V., Stoothoff, W.H., 2004. Tau phosphorylation in neuronal cell function and dysfunction. J. Cell Sci. 117 (Pt 24), 5721–5729.
Jones, L., Holmans, P.A., Hamshere, M.L., Harold, D., Moskvina, V., Ivanov, D., Pocklington, A., Abraham, R., Hollingworth, P., Sims, R., Gerrish, A., Pahwa, J.S., Jones, N., Stretton, A., Morgan, A.R., Lovestone, S., Powell, J., Proitsi, P., Lupton, M.K., Brayne, C., Rubinsztein, D.C., Gill, M., Lawlor, B., Lynch, A., Morgan, K., Brown, K.S., Passmore, P.A., Craig, D., McGuinness, B., Todd, S., Holmes, C., Mann, D., Smith, A.D., Love, S., Kehoe, P.G., Mead, S., Fox, N., Rossor, M., Collinge, J., Maier, W., Jessen, F., Schurmann, B., Heun, R., Kolsch, H., van den Bussche, H., Heuser, I., Peters, O., Kornhuber, J., Wiltfang, J., Dichgans, M., Frolich, L., Hampel, H., Hull, M., Rujescu, D., Goate, A.M., Kauwe, J.S., Cruchaga, C., Nowotny, P., Morris, J.C., Mayo, K., Livingston, G., Bass, N.J., Gurling, H., McQuillin, A., Gwilliam, R., Deloukas, P., Al-Chalabi, A., Shaw, C.E., Singleton, A.B., Guerreiro, R., Muhleisen, T.W., Nothen, M.M., Moebus, S., Jockel, K.H., Klopp, N., Wichmann, H.E., Ruther, E., Carrasquillo, M.M., Pankratz, V.S., Younkin, S.G., Hardy, J., O'Donovan, M.C., Owen, M.J., Williams, J., 2010. Genetic evidence implicates the immune system and cholesterol metabolism in the aetiology of Alzheimer's disease. PLoS One 5, e13950.

Kennedy, N.J., Martin, G., Ehrhardt, A.G., Cavanagh-Kyros, J., Kuan, C.Y., Rakic, P., Flavell, R.A., Treistman, S.N., Davis, R.J., 2007. Requirement of JIP scaffold proteins for NMDA-mediated signal transduction. Genes Dev. 21, 2336–2346.
Kerchner, G.A., Deutsch, G.K., Zeineh, M., Dougherty, R.F., Saranathan, M., Rutt, B.K., 2012. Hippocampal CA1 apical neuropil atrophy and memory performance in Alzheimer's disease. Neuroimage 63, 194–202.
Knopman, D.S., Jack Jr., C.R., Wiste, H.J., Weigand, S.D., Vemuri, P., Lowe, V., Kantarci, K., Gunter, J.L., Senjem, M.L., Ivnik, R.J., Roberts, R.O., Boeve, B.F., Petersen, R.C., 2012. Short-term clinical outcomes for stages of NIA-AA preclinical Alzheimer disease. Neurology 78, 1576–1582.
Knopman, D.S., Jack Jr., C.R., Wiste, H.J., Weigand, S.D., Vemuri, P., Lowe, V.J., Kantarci, K., Gunter, J.L., Senjem, M.L., Mielke, M.M., Roberts, R.O., Boeve, B.F., Petersen, R.C., 2013. Brain injury biomarkers are not dependent on beta-amyloid in normal elderly. Ann. Neurol. 73, 472–480.
Konietzko, U., Goodger, Z.V., Meyer, M., Kohli, B.M., Bosset, J., Lahiri, D.K., Nitsch, R.M., 2010. Co-localization of the amyloid precursor protein and Notch intracellular domains in nuclear transcription factories. Neurobiol. Aging 31, 58–73.
Konietzko, U., 2012. AICD nuclear signaling and its possible contribution to Alzheimer's disease. Curr. Alzheimer Res. 9, 200–216.
Kopeikina, K.J., Polydoro, M., Tai, H.C., Yaeger, E., Carlson, G.A., Pitstick, R., Hyman, B.T., Spires-Jones, T.L., 2013a. Synaptic alterations in the rTg4510 mouse model of tauopathy. J. Comp. Neurol. 521, 1334–1353.
Kopeikina, K.J., Wegmann, S., Pitstick, R., Carlson, G.A., Bacskai, B.J., Betensky, R.A., Hyman, B.T., Spires-Jones, T.L., 2013b. Tau causes synapse loss without disrupting calcium homeostasis in the rTg4510 model of tauopathy. PLoS One 8, e80834.
La Joie, R., Perrotin, A., de La Sayette, V., Egret, S., Doeuvre, L., Belliard, S., Eustache, F., Desgranges, B., Chetelat, G., 2013. Hippocampal subfield volumetry in mild cognitive impairment, Alzheimer's disease and semantic dementia. Neuroimage Clin. 3, 155–162.
Leissring, M.A., Murphy, M.P., Mead, T.R., Akbari, Y., Sugarman, M.C., Jannatipour, M., Anliker, B., Muller, U., Saftig, P., De Strooper, B., Wolfe, M.S., Golde, T.E., LaFerla, F.M., 2002. A physiologic signaling role for the gamma -secretase-derived intracellular fragment of APP. Proc. Natl. Acad. Sci. U. S. A. 99, 4697–4702.
Matsuda, S., Yasukawa, T., Homma, Y., Ito, Y., Niikura, T., Hiraki, T., Hirai, S., Ohno, S., Kita, Y., Kawasumi, M., Kouyama, K., Yamamoto, T., Kyriakis, J.M., Nishimoto, I., 2001. c-Jun N-terminal kinase (JNK)-interacting protein-1b/islet-brain-1 scaffolds Alzheimer's amyloid precursor protein with JNK. J. Neurosci. 21, 6597–6607.
Ohno, N., Kidd, G.J., Mahad, D., Kiryu-Seo, S., Avishai, A., Komuro, H., Trapp, B.D., 2011. Myelination and axonal electrical activity modulate the distribution and motility of mitochondria at CNS nodes of Ranvier. J. Neurosci. 31, 7249–7258.
Oliva Jr., A.A., Atkins, C.M., Copenagle, L., Banker, G.A., 2006. Activated c-Jun N-terminal kinase is required for axon formation. J. Neurosci. 26, 9462–9470.
Orejana, L., Barros-Minones, L., Aguirre, N., Puerta, E., 2013. Implication of JNK pathway on tau pathology and cognitive decline in a senescence-accelerated mouse model. Exp. Gerontol. 48, 565–571.
Pardossi-Piquard, R., Checler, F., 2012. The physiology of the beta-amyloid precursor protein intracellular domain AICD. J. Neurochem. 120 (Suppl 1), 109–124.
Passer, B., Pellegrini, L., Russo, C., Siegel, R.M., Lenardo, M.J., Schettini, G., Bachmann, M., Tabaton, M., D'Adamio, L., 2000. Generation of an apoptotic intracellular peptide by gamma-secretase cleavage of Alzheimer's amyloid beta protein precursor. J. Alzheimers Dis. 2, 289–301.
Pei, J.J., Braak, E., Braak, H., Grundke-Iqbal, I., Iqbal, K., Winblad, B., Cowburn, R.F., 2001. Localization of active forms of C-jun kinase (JNK) and p38 kinase in Alzheimer's disease brains at different stages of neurofibrillary degeneration. J. Alzheimers Dis. 3, 41–48.
Pimplikar, S.W., 2009. Reassessing the amyloid cascade hypothesis of Alzheimer's disease. Int. J. Biochem. Cell Biol. 41, 1261–1268.
Pimplikar, S.W., Nixon, R.A., Robakis, N.K., Shen, J., Tsai, L.H., 2010. Amyloid-independent mechanisms in Alzheimer's disease pathogenesis. J. Neurosci. 30, 14946–14954.
Ponder, C.A., Huded, C.P., Munoz, M.B., Gulden, F.O., Gilliam, T.C., Palmer, A.A., 2008. Rapid selection response for contextual fear conditioning in a cross between C57BL/6J and A/J: behavioral, QTL and gene expression analysis. Behav. Genet. 38, 277–291.
Reynolds, C.H., Utton, M.A., Gibb, G.M., Yates, A., Anderton, B.H., 1997. Stress-activated protein kinase/c-jun N-terminal kinase phosphorylates tau protein. J. Neurochem. 68, 1736–1744.
Robinson, A., Grosgen, S., Mett, J., Zimmer, V.C., Haupenthal, V.J., Hundsdorfer, B., Stahlmann, C.P., Slobodskoy, Y., Muller, U.C., Hartmann, T., Stein, R., Grimm, M.O., 2014. Upregulation of PGC-1alpha expression by Alzheimer's disease-associated pathway: presenilin 1/amyloid precursor protein (APP)/intracellular domain of APP. Aging Cell 13, 263–272.
Ryan, K.A., Pimplikar, S.W., 2005. Activation of GSK-3 and phosphorylation of CRMP2 in transgenic mice expressing APP intracellular domain. J. Cell Biol. 171, 327–335.
Scheinfeld, M.H., Roncarati, R., Vito, P., Lopez, P.A., Abdallah, M., D'Adamio, L., 2002. Jun NH2-terminal kinase (JNK) interacting protein 1 (JIP1) binds the cytoplasmic domain of the Alzheimer's beta-amyloid precursor protein (APP). J. Biol. Chem. 277, 3767–3775.
Scheinfeld, M.H., Matsuda, S., D'Adamio, L., 2003. JNK-interacting protein-1 promotes transcription of A beta protein precursor but not A beta precursor-like proteins, mechanistically different than Fe65. Proc. Natl. Acad. Sci. U. S. A. 100, 1729–1734.
Selkoe, D.J., 2002. Alzheimer's disease is a synaptic failure. Science 298, 789–791.
Selkoe, D.J., 2008. Biochemistry and molecular biology of amyloid beta-protein and the mechanism of Alzheimer's disease. Handbook Clin. Neurol. 89, 245–260.
Shen, J., Kelleher 3rd, R.J., 2007. The presenilin hypothesis of Alzheimer's disease: evidence for a loss-of-function pathogenic mechanism. Proc. Natl. Acad. Sci. U. S. A. 104, 403–409.
Shoji, M., Iwakami, N., Takeuchi, S., Waragai, M., Suzuki, M., Kanazawa, I., Lippa, C.F., Ono, S., Okazawa, H., 2000. JNK activation is associated with intracellular beta-amyloid accumulation. Brain Res. Mol. Brain Res. 85, 221–233.
Son, Y., Kim, S., Chung, H.T., Pae, H.O., 2013. Reactive oxygen species in the activation of MAP kinases. Methods Enzymol. 528, 27–48.
Storandt, M., Head, D., Fagan, A.M., Holtzman, D.M., Morris, J.C., 2012. Toward a multifactorial model of Alzheimer disease. Neurobiol. Aging 33, 2262–2271.
Terry, R.D., Masliah, E., Salmon, D.P., Butters, N., DeTeresa, R., Hill, R., Hansen, L.A., Katzman, R., 1991. Physical basis of cognitive alterations in Alzheimer's disease: synapse loss is the major correlate of cognitive impairment. Ann. Neurol. 30, 572–580.
Vogt, D.L., Thomas, D., Galvan, V., Bredesen, D.E., Lamb, B.T., Pimplikar, S.W., 2011. Abnormal neuronal networks and seizure susceptibility in mice overexpressing the APP intracellular domain. Neurobiol. Aging 32, 1725–1729.
Whitmarsh, A.J., Kuan, C.Y., Kennedy, N.J., Kelkar, N., Haydar, T.F., Mordes, J.P., Appel, M., Rossini, A.A., Jones, S.N., Flavell, R.A., Rakic, P., Davis, R.J., 2001. Requirement of the JIP1 scaffold protein for stress-induced JNK activation. Genes Dev. 15, 2421–2432.
Yoon, S.O., Park, D.J., Ryu, J.C., Ozer, H.G., Tep, C., Shin, Y.J., Lim, T.H., Pastorino, L., Kunwar, A.J., Walton, J.C., Nagahara, A.H., Lu, K.P., Nelson, R.J., Tuszynski, M.H., Huang, K., 2012. JNK3 perpetuates metabolic stress induced by Aβ peptides. Neuron 75, 824–837.
Zempel, H., Thies, E., Mandelkow, E., Mandelkow, E.M., 2010. Abeta oligomers cause localized Ca(2+) elevation, missorting of endogenous Tau into dendrites, Tau phosphorylation, and destruction of microtubules and spines. J. Neurosci. 30, 11938–11950.
Zhang, B., Gaiteri, C., Bodea, L.G., Wang, Z., McElwee, J., Podtelezhnikov, A.A., Zhang, C., Xie, T., Tran, L., Dobrin, R., Fluder, E., Clurman, B., Melquist, S., Narayanan, M., Suver, C., Shah, H., Mahajan, M., Gillis, T., Mysore, J., MacDonald, M.E., Lamb, J.R., Bennett, D.A., Molony, C., Stone, D.J., Gudnason, V., Myers, A.J., Schadt, E.E., Neumann, H., Zhu, J., Emilsson, V., 2013. Integrated systems approach identifies genetic nodes and networks in late-onset Alzheimer's disease. Cell 153, 707–720.
Zhu, X., Raina, A.K., Rottkamp, C.A., Aliev, G., Perry, G., Boux, H., Smith, M.A., 2001. Activation and redistribution of c-jun N-terminal kinase/stress activated protein kinase in degenerating neurons in Alzheimer's disease. J. Neurochem. 76, 435–441.